

Geomorphometry and Spatial Hydrologic Modelling

S.D. Peckham

how can DEMs be used for spatial hydrologic modelling? · what methods are commonly used to model hydrologic processes in a watershed? · what kinds of preprocessing tools are typically required? · what are some of the key issues in spatial hydrologic modelling?

1. INTRODUCTION

Spatial hydrologic modelling is one of the most important applications of the geomorphometric concepts discussed in this book. The simple fact that flow paths follow the topographic gradient results in an intimate connection between geomorphometry and hydrology, and this connection has driven much of the progress in the field of geomorphometry. It also continues to help drive the development of new technologies for creating high-quality and high-resolution DEMs, such as LiDAR. Like most other types of physically-based models, hydrologic models are built upon the fundamental principle that the mass and momentum of water must be conserved as it moves from place to place, whether it is on the land surface, below the surface or evaporating into the atmosphere. While this sounds like a simple enough idea, it provides a powerful constraint that makes predictive modelling possible. When mass and momentum conservation is similarly applied to sediment, it is possible to create *landscape evolution models* that predict the spatial erosion and deposition of sediment and contaminants.

While hydrologic models have been around for several decades, it is only in the last fifteen years or so that computers have become powerful enough for fully spatial hydrologic models to be of practical use. *Spatially-distributed* hydrologic models treat every grid cell in a DEM as a control volume which must conserve both mass and momentum as water is transported to, from, over and below the land surface. The control volume concept itself is quite simple: what flows in must either flow out through another face or accumulate or be consumed in the interior. Conversely, the amount that flows out during any given time step cannot

exceed the amount that flows in during that time step plus the amount already stored inside. However, the number of grid cells required to adequately resolve the transport within a river basin, in addition to the small size of the timesteps required for a spatial model to be numerically stable, results in a computational cost that until recently was prohibitive.

REMARK 1. *Since flow paths follow the topographic gradient, there is an intimate connection between geomorphometry and hydrology. Spatial hydrologic models make use of several DEM-derived grids especially grids of slope, aspect (flow direction) and contributing area.*

For a variety of reasons, including the computational cost of fully spatial models and the fact that data required for more advanced models is often unavailable, researchers have invested a great deal of effort into finding ways to simplify the problem. This has resulted in many different types of hydrologic models. For example, *lumped models* employ a small number of “*representative units*” (very large, but carefully-chosen control volumes), with simple methods to route flow between the units. Another strategy for reducing the complexity of hydrologic models is to use concepts such as *hydrologic similarity* to essentially collapse the 2D (or 3D) problem to a 1D problem. For example, TOPMODEL (Beven and Kirkby, 1979) defines a *topographic index* or *wetness index* and then lumps all grid cells with the same value of this index together under the assumption that they will have the same hydrologic response. Similarly, many models lump together all grid cells with the same elevation (via the *hypsothetic curve* or *area–altitude function*) to simplify the problem of computing certain quantities such as snowmelt. All grid cells with a given *flow distance* to a basin outlet can also be lumped together (via the *width function* or *area–distance function*) and this is the main idea behind the concept of the *instantaneous unit hydrograph*. While models such as these can be quite useful and require less input data, they all employ simplifying assumptions that prevent them from addressing general problems of interest. In addition, these assumptions are often difficult to check and are therefore a source of uncertainty. In essence, these types of models gain their speed by mapping many different (albeit similar) 3D flow problems to the same 1D problem in the hope that the lost differences don’t matter much. While geomorphometric grids are used to prepare input data for virtually all hydrologic models, fully spatial models make direct use of these grids. For this reason, and in order to limit the scope of the discussion, this chapter will focus on fully-spatial models.

There are now many different spatial hydrologic models available, and their popularity, sophistication and ease-of-use continues to grow with every passing year. A few representative examples of some highly-developed spatial models are: *Mike SHE* (a product of Danish Hydraulics Institute, Denmark), *Gridded Surface Subsurface Hydrologic Analysis (GSSHA)*, *CASC2D* (Julien et al., 1995; Ogden and Julien, 2002), *PRMS* (Leavesley et al., 1991), *DHVS* (Wigmosta et al., 1994) and *TopoFlow*. Rather than attempt to review or compare various models, the main goal

of this chapter is to discuss basic concepts that are common to virtually all spatial hydrologic models.

REMARK 2. *Hydrologic processes in a watershed (e.g. snowmelt) may be modelled with either simple methods (e.g. degree-day) or very sophisticated methods (e.g. energy-balance), based partly on the input data that is available.*

It will be seen throughout this chapter that grids of elevation, slope, aspect and contributing area all play fundamental roles in spatial hydrologic modelling. Some of these actually play multiple roles. For example, slope and aspect are needed to determine the velocity of surface (and subsurface) flow, but also determine the amount of solar radiation that is available for evapotranspiration and melting snow. The DEM grid spacing that is required depends on the application, but as a general rule should be sufficient to adequately resolve the local hillslope scale. This scale marks the transition in process dominance from hillslope processes to channel processes. It is typically between 10 and 100 m, but may be larger for arid regions. As a result of the Shuttle Radar Topography Mission (SRTM), DEMs with a grid spacing less than 100 m are now available for much of the Earth. In addition, LiDAR DEMs with a grid spacing less than 10 m can now be purchased from private firms for specific areas. Many of the DEMs produced by government agencies (e.g. the U.S. Geological Survey and Geoscience Australia) now use an algorithm such as ANUDEM (Hutchinson, 1989) to produce “hydrologically sound” DEMs which makes them better suited to hydrologic applications (see also Section 3.2 in Chapter 2).

This chapter has been organised as follows. Section 2 discusses several key hydrologic processes and how they are typically incorporated into spatial models. Note that spatial hydrologic models integrate many branches of hydrology and there are many different approaches for modelling any given process, from simple to very complex. It is therefore impossible to give a complete treatment of this subject in this chapter. For a greater level of detail the reader is referred to textbooks and monographs such as Henderson (1966), Eagleson (1970), Freeze and Cherry (1979), Welty et al. (1984), Beven (2000), Dingman (2002), Smith (2002). The goal here is to highlight the most fundamental concepts that are common between spatial models and to show how they incorporate geomorphometric grids. Section 3 discusses scale issues in spatial hydrologic modelling. Section 4 provides a brief discussion of preprocessing tools that are typically needed in order to prepare required input data. Section 5 is a simple case study in which a model called TopoFlow is used to simulate the hydrologic response of a small ungauged watershed in the Baranja Hill case study.

2. SPATIAL HYDROLOGIC MODELLING: PROCESSES AND METHODS

2.1 The control volume concept

Spatially-distributed hydrologic models are based on applying the control volume concept to every grid cell in a digital elevation model (DEM). It is helpful to imagine a box-shaped control volume resting on the land surface such that its top and

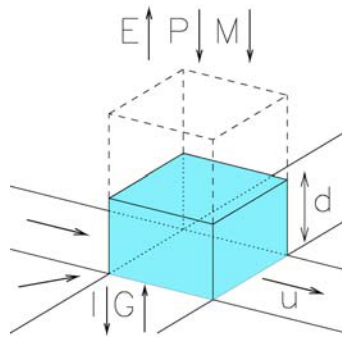


FIGURE 1 A grid-cell control volume resting on the land surface and filled with water to a depth, d . Precipitation, P , snowmelt, M , evapotranspiration, E , infiltration, I , and groundwater seepage, G add or remove water from the top and bottom faces, while surface water flows through the four vertical faces. Overland flow is shown, but a grid cell may instead contain a single, sinuous channel with a width less than the grid spacing.

bottom faces have the x and y dimensions of a DEM grid cell and such that the height of the box is greater than the local water depth (see Figure 1). Water flowing from cell to cell across the land surface flows horizontally through the four vertical faces of this box, according to the D8, D-Infinity or Mass Flux method (see Section 3.2 in Chapter 7). For overland flow, the entire bottom of the box may be wetted and 2D modelling of the flow is possible. For channelised flow, the grid cell dimensions are typically much larger than the channel width, so channel width must be specified as a separate grid, along with an appropriate sinuosity in order to properly compute mass and momentum balance.

Runoff-generating processes can be thought of as “injecting” flow vertically through the top face of the box, as in the case of rainfall and snowmelt, or through the bottom of the box, as in the case of seepage from the subsurface as a result of the local water table rising to the surface. Similarly, infiltration and evapotranspiration are vertical flux processes that result in a loss of water through either the bottom or top faces of the box, respectively. If a grid cell contains a channel, then the volume of surface water stored in the box depends on the channel dimensions and water depth, d , otherwise it depends on the grid cell dimensions and water depth.

The net vertical flux into the box may be referred to as the *effective rainrate*, R , and is the runoff that was generated within the box. It is given by the equation:

$$R = (P + M + G) - (E + I) \quad (2.1)$$

where P is the precipitation rate, M is snowmelt rate, G is the rate of subsurface seepage, E is the evapotranspiration rate and I is the infiltration rate.

Each of these six quantities varies both spatially and in time and is therefore stored as a grid of values that change over time. Each also has units of [mm/hr]. Methods for computing these quantities are outlined in the next few subsections of this chapter. Note that the total runoff from the box is not equivalent to the effective rainrate because it consists of the effective rainrate *plus* any amount that

flowed horizontally into the box and was not consumed by infiltration or evapotranspiration. Note also that in order to model the details of subsurface flow, it is necessary to work with an additional “stack” of boxes that extend down into the subsurface; e.g. there may be one such box for each of several soil layers.

In many models of fluid flow, fluxes through control volume boundaries (e.g. the vertical faces of the box) are not computed directly. Instead, the boundary integrals are converted to integrals over the interior of the box using the well-known *divergence theorem* (Wety et al., 1984). This results in differential vs. integral equations and requires computing first and second-order spatial derivatives between neighbouring cells, typically via finite-difference methods. However, if we assume that flow directions are determined by topography, which is a relatively static quantity, then flow directions between grid cells are fixed and known at the start of a model run. Under these circumstances it is straight-forward and efficient to compute boundary integrals.

2.2 The precipitation process

The precipitation process differs from most of the other hydrologic processes at work in a basin in that the precipitation rate must be specified either from measurements (e.g. radar or rain gauges) or as the result of numerical simulation. All of the other processes are concerned with methods for tracking water that is already in the system as it moves from place to place (e.g. cell to cell or between surface and subsurface). For a small catchment, it may be appropriate to use measured rainrates from a single gauge for all grid cells. For larger catchments and greater realism, however, it is better to use space-time rainfall, which is stored as a grid stack, indexed by time. This grid stack may be created by spatially interpolating data from many different rain gauges. Input data for air temperature (T) is used to determine whether precipitation falls as rain or as snow.

In order to model how temperature decreases with increasing elevation, a grid of elevations can be used together with a lapse rate. If precipitation falls as snow ($T < 0^\circ\text{C}$), then it can be stored as a grid of snow depths that can change in time. If the snowmelt process is modelled, then snowmelt can contribute runoff to any grid cell that has a nonzero snow depth and an air temperature greater than 0°C .

2.3 The snowmelt process

In general, the conversion of snow to liquid water is a complex process that involves a detailed exchange of energy in its various forms between the atmosphere and the snowpack. While air temperature is obviously of key importance, numerous other variables affect the meltrate, including the slope and aspect of the topography, wind speed and direction, the heights of roughness elements (e.g. vegetation) and the snow density to name a few. The *Energy-Balance Method* (Marks and Dozier, 1992; Liston, 1995; Zhang et al., 2000) in its various implementations is therefore the most sophisticated method for melting snow, but it is very data intensive. This method consists of numerous equations (see references) and generally makes use of a clear-sky radiation model (see Section 3.1 in Chapter 8; Dozier,

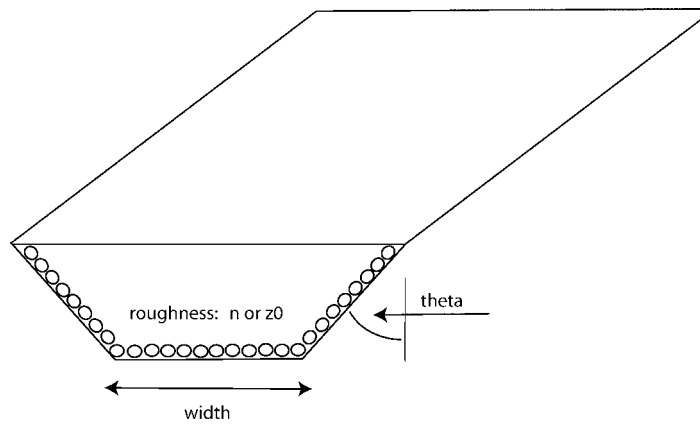


FIGURE 2 A channel with a trapezoidal cross-section and roughness elements that would connect the centres of two DEM grid cells. The cross-section becomes triangular when the bed width is zero and rectangular when the bank angle is zero.

1980, or Dingman, 2002, Appendix E), for modelling the shortwave solar radiation and the *Stephan–Boltzmann law* for modelling the longwave radiation. Most clear-sky radiation models incorporate topographic effects via slope and aspect grids extracted from DEMs.

Since the input data required for energy balance calculations is only available in well-instrumented watersheds, much simpler methods for estimating the rate of snowmelt have been developed such as various forms of the well-known *Degree-Day Method* (Beven, 2000, p. 80). The basic method predicts the melt rate using the simple formula:

$$M = c_0 \cdot \Delta T \quad (2.2)$$

where ΔT is the temperature difference between the air and the snow and c_0 is an empirical coefficient with units of [mm/hr/°C]. In both the Degree-Day and Energy-Balance methods it is possible for any input variable to vary spatially and in time, and many authors suggest that c_0 should vary throughout the melt season. An example comparison of these two methods is given by Bathurst and Cooley (1996). Whatever method is used, the end result is a grid sequence of snowmelt rates, M , that is then used in Equation (2.1).

2.4 The channel flow process

Spatial hydrologic models are based on conservation of mass and momentum, and many of them make direct use of D8 flow direction grids and slope grids to compute the amount of mass and momentum that flows into and out of each grid cell. The grid cell size is generally chosen to be smaller than the hillslope scale and larger than the width of the largest channel (see Section 3). Every grid cell then has one channel associated with it that extends from the centre of the grid cell to the

centre of the grid cell that it flows to according to the D8 method. Channelised flow is then modelled as an essentially 1D process (in a treelike network of channels), while recognising that it will be necessary to store additional channel properties for every grid cell such as:

- sinuosity or channel length;
- channel bed width;
- bank angle (if trapezoidal cross sections are used) and;
- a channel roughness parameter.

One method for creating these channel property grids is discussed in Section 4.

The *kinematic wave* method is the simplest method for modelling flow in open channels and is available as an option in virtually all spatial hydrologic models. This method combines mass conservation with the simplest possible treatment of momentum conservation, namely that all terms in the general momentum equation (pressure gradient, local acceleration and convective acceleration) are negligible except the friction and gravity terms. In this case the water surface slope, energy slope and bed slope are all equal. In addition, the balance of gravity against friction (as a shear stress near the bed) results in an equation for depth-averaged flow velocity, u , in terms of the flow depth, d , bed slope (rise over run), S , and a roughness parameter. If the shear stress near the bed is computed using our best theoretical understanding of turbulent boundary layers (Schlichting, 1960), then this balance results in the *law of the wall*:

$$u = (g \cdot R_h \cdot S)^{1/2} \cdot \ln\left(a \cdot \frac{d}{z_0}\right) \cdot \kappa^{-1} \quad (2.3)$$

Here, g is the gravitational constant, R_h is the *hydraulic radius*, given as the ratio of the wetted cross-sectional area and wetted perimeter (units of length), a is an integration constant (given by 0.368 or 0.476, depending on the formulation), z_0 is the *roughness height* (units of length), and $\kappa \approx 0.408$ is von Karman's constant.

Note that the law of the wall is general and is also used by the snowmelt energy-balance models for modelling air flow in the atmospheric boundary layer. However, in the setting of open-channel flow, an alternative known as *Manning's formula* is more often used. Manning's formula, which was determined by fitting a power-law to data gives the depth-averaged velocity as:

$$u = \frac{R_h^{2/3} \cdot S^{1/2}}{n} \quad (2.4)$$

where n is an empirical roughness parameter with the units of $[s/m^{1/3}]$ required to make the equation dimensionally consistent. Manning's formula agrees very well with the law of the wall as long as the relative roughness, z_0/d is between about 10^{-2} and 10^{-4} . This is the range that is encountered in most open-channel flow problems. Smaller relative roughnesses are typically encountered in the case where wind blows over terrain and vegetation. ASCE Task Force on Friction Factors (1963) provides a good review of the long and interesting history that led to Equations (2.3) and (2.4).

While the kinematic wave method is an approximation, it often yields good results, especially when slopes are steep. The *diffusive wave* method provides a somewhat better approximation by retaining one additional term in the momentum equation, namely the pressure-gradient (water depth derivative) term. In this method, the slope of the free water surface is used instead of the bed slope, and pressure-related (e.g. backwater) effects can be modelled. Note that a general treatment of momentum conservation uses the full *St. Venant equation*, which includes the effects of gravity, friction and pressure-gradients as well as terms for local and convective acceleration. The convective acceleration term corresponds to the net flux of momentum into a given control volume. The most accurate but most computationally demanding approach retains all of the terms in the St. Venant equation and is known as the *dynamic wave* method. Interestingly, the latter two methods create a water-depth gradient and can thereby move water across flat areas (e.g. lakes) in a DEM. These areas have a bed slope of zero and therefore receive a velocity of zero in the kinematic wave method unless they are handled separately in some manner. Whether the kinematic, diffusive or dynamic wave method is used, it is necessary to compute a grid of bed slopes. Given a DEM with sufficient vertical resolution, the bed slope can be computed between each grid cell and its downstream neighbour, as indicated by a D8 flow grid (see Chapter 7).

The D8 flow direction grid indicates the (static) connectivity of the grid cells in a DEM and can therefore be used directly to simplify mass and momentum balance calculations. A D8 flow grid allows fluxes across grid cell boundaries to be computed, which makes it possible to use integral equations instead of differential equations (Welty et al., 1984). In particular, the use of integral equations is simpler because convective acceleration (momentum flux) between cells can be modelled without computing spatial derivatives. Grids for the initial flow depth, d , and velocity, u , are specified, either as all zeros or computed from channel properties and a base-level recharge rate. Given the cross-sectional shape (e.g. trapezoidal) and length, L , of each channel, the volume of water in the channel can be computed as $V = A_c \cdot L$, where A_c is the cross-sectional area. An outgoing discharge, $Q = u \cdot A_c$, can also be computed for every grid cell. For each time step, the change in volume $V(i, t)$ for pixel i can then be computed as:

$$\Delta V(i, t) = \Delta t \cdot \left[R(i, t) \cdot \Delta x \cdot \Delta y - Q(i, t) + \sum_{k \in N} Q(k, t) \right] \quad (2.5)$$

where R is the excess rainrate computed from Equation (2.1), Δx and Δy are the pixel dimensions, $Q(i, t)$ is the outgoing discharge from pixel i at time t , and the summation is over all of the neighbour pixels that have D8-flow into pixel i .

Once Equation (2.5) has been used to update V for each pixel, the grid of flow depths, d , can be updated using the channel geometry grids that give the length, bed width and bank angle of each channel. In the case of the kinematic wave approximation, the grids d and S can then be used to update the grid of flow velocities, u , using either Equation (2.3) or Equation (2.4). For an integral-equation version of the dynamic wave method, the velocity grid, $u(i, t)$, would be incre-

mented by an amount:

$$\begin{aligned} \Delta u(i, t) = & \left(\frac{\Delta t}{d(i, t) \cdot A_w} \right) \cdot \left\{ u(i, t) \cdot Q(i, t) \cdot (C - 1) \right. \\ & + \sum_{k \in N} [u(k, t) - u(i, t) \cdot C] \cdot Q(k, t) \\ & - u(i, t) \cdot C \cdot R(i, t) \cdot \Delta x \cdot \Delta y \\ & \left. + A_w \cdot [g \cdot d(i, t) \cdot S(i, t) - f(i, t) \cdot u^2(i, t)] \right\} \end{aligned} \quad (2.6)$$

where A_w is the wetted surface area of the bed, A_t is the top surface area of the channel and $C = A_w/A_t$. For overland grid cells, $C = 1$, and for channel grid cells $C > 1$. A_w and A_t are computed from the grid of channel lengths, L , and the assumed cross-sectional shape. In the last term, $f \equiv \tau_b/(\rho \cdot u^2)$ is a dimensionless friction factor:

$$f = \left[\frac{\kappa}{\ln(a \cdot \frac{d}{z_0})} \right]^2 \quad (2.7)$$

which corresponds to the law of the wall, while $f = g \cdot n^2 \cdot R_h^{-1/3}$ corresponds to Manning's equation. Instead of using the bed slope for S in Equation (2.6), the water surface slope would be computed from the DEM, d and the D8 flow direction grid. As the numerical approach shown here is *explicit*, numerical stability requires a small enough time step such that water cannot flow across any grid cell in less than one time step. If u_m is the maximum velocity, then we require $\Delta t < \Delta x/u_m$ for stability.

2.5 The overland flow process

The fundamental concept of *contributing area* was introduced in previous chapters (see Chapter 7). Grid cells with a sufficiently large contributing area will tend to have higher and more persistent surface fluxes and channelised flow. Conversely, grid cells with small contributing areas will tend to have lower, intermittent fluxes. The intermittent nature of runoff-generating events, and the increased likelihood that small amounts of water will be fully consumed by infiltration or evapotranspiration make it even more likely that grid cells with small contributing areas will have little or no surface flux for much of the time. In addition, the *relative roughness* of the surface (typical height of roughness elements divided by the water depth) is higher for smaller contributing areas so that frictional processes will be more efficient at slowing the flow. Under these circumstances the shear stress¹ on the land-surface will tend to be too small to carve a channel or too infrequent to maintain a channel.

Any surface flux will be as so-called *overland* or *Hortonian* flow and will tend to flow in a sheet that wets the entire bottom surface of a grid cell control volume

¹ Proportional to the square of the flow velocity.

during an event. This flow may be modelled with either a 1D or 2D approach, where the latter method would be required to model flood events that exceed the bankfull channel depth, e.g. a dam break. In this case both channelised and overland flow must be modelled for channel grid cells.

Some models, such as CASC2D (Julien and Sagharian, 1991) have a *retention depth* (surface storage) that must be exceeded before overland flow begins. Note that for sheet flow, the hydraulic radius, R_h is very closely approximated by the flow depth, d . If w is the width of the grid cell projected in the direction of the flow, then the wetted area is given by $w d$ and the “*wetted perimeter*” is given by w . It follows that the hydraulic radius is equal to d . It has been found by Eagleson (1970) and many others since that Manning-type equations can be used to compute the flow velocity for overland flow, but that a very large “Manning’s n ” value of around 0.3 or higher is required, versus a typical value of 0.03 for natural channels.

2.6 The evaporation process

Evaporation is a complex, essentially vertical process that moves water from the Earth’s surface and subsurface to the atmosphere. As with the snowmelt process, the most sophisticated approach is based on a full surface energy balance in which topographic effects can be incorporated by including grids of slope and aspect in the solar radiation model. However, since much of the required input data is typically unavailable, a number of simpler models have been proposed. The *Priestley–Taylor* (Priestley and Taylor, 1972; Rouse and Stewart, 1972; Rouse et al., 1977; Zhang et al., 2000) and *Penman–Monteith* models (Beven, 2000; Dingman, 2002) and their variants are two simplified approaches that are used widely. Sumner and Jacobs (2005) provide a comparison of these and other methods.

Whatever method is used, the end result is a grid sequence of evapotranspiration rates, E , that is then used in Equation (2.1). Some distributed hydrologic models have additional routines for modelling the amount of water that is moved from the root zone of the subsurface to the atmosphere by the transpiration of plants. A separate submodel is sometimes used to model the variation of soil temperature with depth, especially for high-latitude applications.

2.7 The infiltration process

The process of infiltration is also primarily vertical, but is arguably the most complex hydrologic process at work in a basin. It has a first-order effect on the hydrologic response of watersheds, and is central to problems involving surface soil moisture. It operates in the *unsaturated zone* between the surface and the water table and represents an interplay between absorption due to capillary action and the force of gravity. A variety of factors make realistic modelling of infiltration difficult, including the nature of boundary conditions at the surface, between soil layers and at the water table (a moving boundary). Variables such as hydraulic conductivity can vary over orders of magnitude in both space and time and the equations are strongly nonlinear.

As pointed out by many authors, including Smith (2002), it is generally not sufficient to simply use spatial averages for input parameters, and best methods for parameter estimation are an active area of research. So-called macropores may be present and must then be modelled separately since they do not conform to the standard notion of a porous medium. Discontinuous permafrost may also be present in high-latitude watersheds. Smith (2002) provides an excellent reference for infiltration theory, ranging from very simple to advanced approaches.

Most spatial hydrologic models use a variant of the *Green-Ampt* or *Smith-Parlange* method for modelling infiltration (Smith, 2002). However, these are simplified approaches that are intended for the relatively simple case where there is:

- a single storm event,
- a single soil layer and
- no water table.

While they can be useful for predicting flood runoff, they are not able to address many other problems of contemporary interest, such as:

- (1) redistribution of the soil moisture profile between runoff-producing events,
- (2) drying of surface layers due to evaporation at the surface,
- (3) rainfall rates less than K_s (saturated hydraulic conductivity),
- (4) multiple soil layers with different properties, and
- (5) the presence of a dynamic water table.

In order to address these issues and to model surface soil moisture a more sophisticated approach is required.

Infiltration in a porous medium is modelled with four basic quantities which vary spatially throughout the subsurface and with time. The *water content*, θ , is the fraction of a given volume of the porous medium that is occupied by water, and must therefore always be less than the *porosity*, ϕ . In the case of soils, θ represents the *soil moisture*. The *pressure head* (or capillary potential), ψ , is negative in the unsaturated zone and measures the strength of the capillary action. It is zero at the water table and positive below it. The *hydraulic conductivity*, K , has units of velocity and depends on the gravitational constant, the density and viscosity of water and the intrinsic permeability of the porous medium.

Darcy's Law, which serves as a good approximation for both saturated and unsaturated flow, implies that the vertical flow rate, v , is given by:

$$v = -K \cdot \frac{dH}{dz} = K \cdot \left(1 - \frac{d\psi}{dz} \right) \quad (2.8)$$

since $H = \psi - z$ (and z is positive downward). Conservation of mass for this problem takes the form:

$$\frac{\partial \theta}{\partial t} + \frac{\partial v}{\partial z} = J \quad (2.9)$$

where J is an optional source/sink term that can be used to model water extracted by plants. Inserting Equation (2.8) into Equation (2.9) we obtain *Richards' equation*:

$$\frac{\partial \theta}{\partial t} = \frac{\partial}{\partial z} \left[K \cdot \left(\frac{\partial \psi}{\partial z} - 1 \right) \right] \quad (2.10)$$

for vertical, one-dimensional unsaturated flow. Many spatial models solve this equation numerically to obtain a profile of soil moisture vs. depth for every grid cell, between the surface and a dynamic water table. However, in order to solve for the four variables, θ , ψ , K and v , two additional equations are required in addition to Equations (2.8) and (2.9). These extra equations have been determined empirically by extensive data analysis and are called *soil characteristic functions*.

The soil characteristic functions most often used are those of Brooks and Corey (1964), van Genuchten (1980) and Smith (1990). Each expresses K and ψ as functions of θ and contains parameters that depend on the porous medium under consideration (e.g. sand, silt, or loam).

The *transitional Brooks–Corey method* combines key advantages of the Brooks–Corey and van Genuchten methods (Smith, 1990, 2002, pp. 18–23). Water content, θ , is first rescaled to define a quantity called the *effective saturation*:

$$\Theta_e = \frac{\theta - \theta_r}{\theta_s - \theta_r} \quad (2.11)$$

that lies between zero and one. Here, θ_s is the *saturated water content* (slightly less than the porosity, ϕ) and θ_r is the *residual water content* (a lower limit that cannot be lowered via pressure gradients). Hydraulic conductivity is then modelled as:

$$K = K_s \cdot \Theta_e^\epsilon \quad (2.12)$$

where K_s is the *saturated hydraulic conductivity* (an upper bound on K) and $\epsilon = (2 + 3\lambda)/\lambda$, where λ is the *pore size distribution parameter*. Pressure head is modelled as:

$$\psi = \psi_B \cdot [\Theta_e^{-c/\lambda} - 1]^{1/c} - \psi_a \quad (2.13)$$

where ψ_B is the *bubbling pressure* (or *air-entry tension*, ψ_a is a small shift parameter (which may be used to approximate hysteresis or set to zero), c is the *curvature parameter* which determines the shape of the curve near saturation.

Equations (2.8), (2.9), (2.12) and (2.13) provide a very flexible basic framework for modelling 1D infiltration in spatial hydrologic models. The precipitation rate, P , the snowmelt rate, M , and evapotranspiration rate, E , are needed for the upper boundary condition. The vertical flow rate computed at the surface, v_0 , determines I in Equation (2.1).

2.8 The subsurface flow process

Once infiltrating water reaches the water table, the hydraulic gradient is such that it typically begins to move horizontally, roughly parallel to the land surface. The water table height may rise or fall depending on whether the net flux is downward (infiltration) or upward (exfiltration, due to evapotranspiration). Darcy's law [Equation (2.8)] continues to hold but $K = K_s$, $\theta = \theta_s \approx \phi$ and $\psi = 0$ at the water table, with hydrostatic conditions ($\psi > 0$) below it. More details on the equations used to model saturated flow are given by Freeze and Cherry (1979).

For shallow subsurface flow, various simplifying assumptions are often applicable, such as (1) the subsurface flow direction is the same as the surface flow

direction and (2) the porosity decreases with depth. Under these circumstances the water table height can be modelled as a grid that changes in time, using a control volume below each DEM grid cell that extends from the water table down to an impermeable lower surface (e.g. bedrock layer). Infiltration then adds water just above the water table at a rate determined from Richard's equation and water moves laterally through the vertical faces at a rate determined by Darcy's law. The dynamic position of the water table is compared to the DEM; if it reaches the surface anywhere, then the rate at which water seeps to the surface provides a grid sequence, G , that is used in Equation (2.1). Multiple layers, each with different hydraulic properties and spatially-variable thickness can be modelled, but this increases the computational cost.

2.9 Flow diversions: sinks, sources and canals

Flow diversions are present in many watersheds and may be modelled as another "process". Man-made canals or tunnels are often used to divert flow from one location to another, and usually cannot be resolved by DEMs. They are typically used for irrigation or urban water supplies. Tunnels may even carry flow from one side of a drainage divide to the other. Given the flow rate at the upstream end and other information such as the length of the diversion, these structures can be incorporated into distributed models. Diversions can be modelled by providing a mechanism (outside of the D8 framework) for transferring water between two non-adjacent grid cells. Sources and sinks may be man-made or natural and simply inject or remove flow from a point location at some rate. If the rate is known, their effect can also be modelled. It is increasingly uncommon to find watersheds that are not subject to human influences.

3. SCALE ISSUES IN SPATIAL HYDROLOGIC MODELS

While the preceding sections may give the impression that spatial hydrologic modelling is simply a straight-forward application of known physical laws, this is far from true. Many authors have pointed out that physically-based mathematical models developed and tested at a particular scale (e.g. laboratory or plot) may be inappropriate or at least gross simplifications when applied at much larger scales. In addition, heterogeneity in natural systems (e.g. rainfall, snowpack, vegetation, soil properties) means that some physical parameters appearing in models may vary considerably over distances that are well below the proposed model scale (grid spacing). It is therefore a nontrivial question as to how (or whether) a small number of "point" measurements can be used to set the parameters of a distributed model. *Variogram analysis* provides one tool for addressing this problem and seeking a correlation length that may help to select an appropriate model scale. For some model parameters, remote sensing can provide an alternative to using point measurements.

The issue of *upscaling*, or how best to move between the measurement scale, process scale and model scale is very important and presents a major research

challenge. A standard approach to this problem that has met with some success is the use of *effective parameters*. The idea is that using a representative value, such as a spatial average, might make it possible to apply a plot-scale mathematical model at the much larger scale of a model grid cell. Unfortunately, the models are usually nonlinear functions of their parameters so a simple spatial average is almost never appropriate. It is well-known in statistics that if X is some model parameter that varies spatially, f is a nonlinear² function and $Y = f(X)$ is a computed quantity, then $E[f(X)] \neq f(E[X])$. Here E is the expected value, akin to the spatial average. So, for example, the mean infiltration rate over a model grid cell (and associated net vertical flux) cannot be computed accurately by simply using mean soil properties (e.g. hydraulic conductivity) in Richards' equation.

An interesting variant of the effective parameter approach is to parameterise the subgrid variability of turbulent flow fields by replacing the molecular viscosity in the time-averaged model equations with an *eddy viscosity* that is allowed to vary spatially. This approach is successfully used by many ocean and climate models and may provide conceptual guidance for hydrologic modelers.

When it comes to the channel network and D8 flow between grid cells, upscaling is even more complicated because there is a fairly abrupt change in process dominance at the *hillslope scale* which marks the transition from overland to channelised flow. As seen in Section 6 of Chapter 7, this scale depends on the region and is needed in the pruning step when extracting a river network from a DEM. If the grid spacing is small enough to resolve the local hillslope scale, then it is possible to classify each grid cell as either hillslope or channel. Each channel grid cell will typically contain a single channel with a width that is less than the grid spacing, as well as some "*hillslope area*". Momentum balance can be modelled as long as channel properties such as length and bed width are stored for each grid cell, and the vertical resolution of the DEM is sufficient to compute the bed slope. However, if the grid spacing is larger than the hillslope scale, then a single grid cell may contain a dendritic network vs. a single channel. This is a much more complicated situation, but it may still be possible to get acceptable results by modelling flow in the cell's dendritic network with a single "*effective*" channel, using effective parameters.

REMARK 3. *Physically-based mathematical models developed and tested at a particular scale (e.g. laboratory or plot) may be inappropriate or at least gross simplifications when applied at much larger scales. The issue of upscaling, or how best to move between the measurement scale, process scale and model scale is very important and represents a major research challenge.*

Using effective parameters and other upscaling methods, researchers have reported successful applications of spatial hydrologic models from the plot scale all the way up to the continental scale. Interestingly, the same model (e.g. MIKE SHE), but with very different parameter settings, can often be used at these two very different scales. While conventional wisdom suggests that traditional, lumped or semi-distributed models are better for large-scale applications, this has been

² Anything other than $a \cdot X + b$.

largely for computational reasons and is becoming less of an issue. Note also that a distributed model is similar in many ways to a lumped model when a large grid spacing is used, although a lumped model may subdivide a watershed into a more natural set of linked control volumes.

Although much more work needs to be done on scaling issues, considerable guidance to modelers is available in the literature. Examples of some good general references include Gupta et al. (1986), Blöschl and Sivapalan (1995), Blöschl (1999a) and Beven (2000). References for specific processes include Dagan (1986) (groundwater), Gupta and Waymire (1993) (rainfall), Wood and Lakshmi (1993) (evaporation and energy fluxes), Peckham (1995b) (channel network geometry and dynamics), Woolhiser et al. (1996) (overland flow), Blöschl (1999b) (snow hydrology) and Zhu and Mohanty (2004) (infiltration).

4. PREPROCESSING TOOLS FOR SPATIAL HYDROLOGIC MODELS

As explained in the previous sections, most spatially-distributed hydrologic models make direct use of a DEM and several DEM-derived grids, including a flow direction grid (aspect), a slope grid and a contributing area grid. Extraction of these grids from a DEM with sufficient vertical and spatial resolution is therefore a necessary first step and may require depression filling or burning in streamlines as already explained in detail in previous chapters (e.g. Chapters 4 and 7). But spatially-distributed models require a fair amount of additional information to be specified for every grid cell before any predictions can be made.

Initial conditions are one type of information that is required. Examples of initial conditions include the initial depth of water, the initial depth of snow, the initial water content (throughout the subsurface) and the initial position of the water table. Each of these examples represents the starting value of a dynamic variable that changes in time. *Channel geometry* is another type of required information, but is given by static variables such as length, bed width, bed slope, bed roughness height and bank angle. Each of these must also be specified for every grid cell or corresponding channel segment. *Forcing variables* are yet another type of information that is required and they are often related to weather. Examples include the precipitation rate, air temperature, humidity, cloudiness, wind speed, and clear-sky solar radiation.

Each type of information discussed above can in principle be measured, but it is virtually impossible to measure them for every grid cell in a watershed. As a result of this fact, these types of measurements are typically only available at a few locations (i.e. stations) as a time series, and interpolation methods (such as the inverse distance method) must be used to estimate values at other locations and times. This important task is generally performed by a preprocessing tool, which may or may not be included with the distributed model.

REMARK 4. *A variety of pre- and postprocessing tools are required to support the use of spatial hydrologic models.*

Another important preprocessing step is to assign reasonable values for channel properties to every spatial grid cell. Some spatial hydrologic models provide a preprocessing tool for this purpose. One method for doing this is to parameterise them as best-fit, power-law functions of contributing area. That is, if A denotes a contributing area grid, then a grid of approximate channel widths can be computed via:

$$w = c \cdot (A + b)^p \quad (4.14)$$

where the parameters c , b and p are determined by a best fit to available data. The same approach can be used to create grids of bed roughness values and bank angles. This approximation is motivated by the well-known *empirical equations of hydraulic geometry* (Leopold et al., 1995) that express hydraulic variables as powers of discharge, and discharge as a power of contributing area. Measurements (e.g. channel widths) to determine best-fit parameters may be available at select locations such as gauging stations, or may be estimated using high-resolution, remotely-sensed imagery.

For an initial condition such as flow depth, an iterative scheme (e.g. Newton–Raphson) can be used to find a steady-state solution given the channel geometry and a baseflow recharge rate; this *normal flow* condition provides a reasonable initial condition. Alternately, a spatial model may be “*spun up*” from an initial state where flow depths are zero everywhere and run until a steady-state baseflow is achieved. Similar approaches could be used to estimate the initial position of the water table. Methods for estimating water table height based on wetness indices have also been proposed (see Section 6 in Chapter 7, Section 4.2 in Chapter 8 and Beven, 2000). Any of these approaches may be implemented as a preprocessing tool.

When energy balance methods are used to model snowmelt or evapotranspiration, it is necessary to compute the net amount of shortwave and longwave radiation that is received by each grid cell. As part of this calculation one needs to compute the *clear-sky solar radiation* as a grid stack indexed by time. The concepts behind computing clear-sky radiation are discussed in Section 3.1 of Chapter 8 and are also reviewed by Dingman (2002, Appendix E). The calculation uses celestial mechanics to compute the declination and zenith angle of the sun, as well as the times of local sunrise and sunset. It also takes the slope and aspect of the terrain into account (as grids), along with several additional variables such as surface albedo, humidity, dustiness, cloudiness and optical air mass. A general approach models direct, diffuse and backscattered radiation.

Another useful type of preprocessing tool is a rainfall simulator. One method for simulating space-time rainfall uses the mathematics of *multifractal cascades* (Over and Gupta, 1996) and reproduces many of the space–time scaling properties of convective rainfall.

It should be noted that DEMs with a vertical resolution of one meter do not permit a sufficiently accurate measurement of channel slope using the standard, local methods of geomorphometry. Channel slopes are often between 10^{-2} and 10^{-5} , but for a DEM with vertical and horizontal resolutions of 1 and 10 meters,

respectively, the minimum resolvable (nonzero) slope is 0.1. The author has developed an experimental “*profile-smoothing*” algorithm for addressing this issue that is available as a preprocessing tool in the TopoFlow model.

5. CASE STUDY: HYDROLOGIC RESPONSE OF NORTH BASIN, BARANJA HILL

As a simple example of how a spatial hydrologic model can be used to simulate the hydrologic response of a watershed, in this section we will apply the TopoFlow model to a small watershed that drains to the northern edge of the Baranja Hill DEM. This is the largest complete watershed in the Baranja Hill DEM, an area in Eastern Croatia that is used for examples throughout this book.

TopoFlow is a free, community-based, hydrologic model that has been developed by the author and colleagues. The TopoFlow project is an ongoing, open-source, collaborative effort between the author and a group of researchers at the University of Alaska, Fairbanks (L. Hinzman, M. Nolan and B. Bolton). This effort began with the idea of merging two spatial hydrologic models into one and adding a user-friendly, point-and-click interface. One of these models was a D8-based, rainfall-runoff model written by the author, which supported both kinematic and dynamic wave routing, as well as both Manning’s formula and the law of the wall for flow resistance. The second model, called ARHYTHM, was written by L. Hinzman and colleagues (Zhang et al., 2000) for the purpose of modelling Arctic watersheds; it therefore contained advanced methods for modelling thermal processes such as snowmelt, evaporation and shallow-subsurface flow. In addition to its graphical user interface, TopoFlow now provides several different methods for modelling infiltration (from Green–Ampt to the 1D Richards’ equation) and also has a rich set of preprocessing tools (Figure 3). Examples of such tools include a rainfall simulator, a data interpolation tool, a channel property assignment tool and a clear-sky solar radiation calculator.

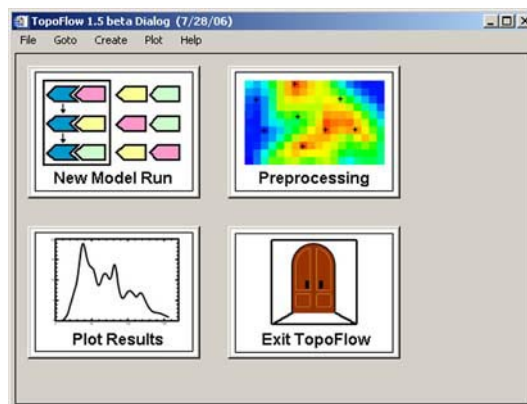


FIGURE 3 The main panel in TopoFlow.

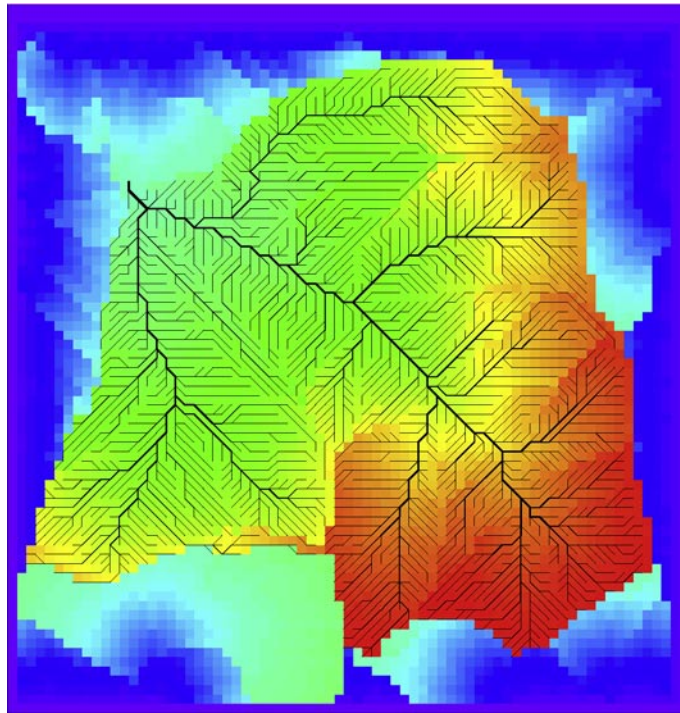


FIGURE 4 Flow lines for the small basin near the north edge of the Baranja DEM, as extracted from a DEM by the D8 method. The flow lines are overlaid on a colour image that shows flow distance to the basin outlet. (See page 755 in Colour Plate Section at the back of the book.)

Before starting *TopoFlow*, *RiverTools* 3.0 (see Chapter 18) was used to clip a small DEM from the Baranja Hill DEM that contained just the north basin. This DEM had only 73 columns and 76 rows, but the same grid spacing of 25 meters. It had minimum and maximum elevations of 85 and 243 meters, respectively. *RiverTools* 3.0 was then used to extract several D8-based grids, including a flow direction grid, a slope grid, a flow distance grid and a contributing area grid. The drainage network above a selected outlet pixel (near the village of Popovac) was also extracted and had a contributing area of 1.84 square kilometers and a fairly large main-channel slope of 0.04 [m/m]. *RiverTools* automatically performs pit-filling when necessary (see Chapter 7) but this was not much of an issue for this DEM because of its relatively steep slopes. Figure 4 shows the D8 flow lines for this small watershed, overlaid on a grid that shows the flow distance to the edge of the bounding rectangle with a rainbow colour scheme.

The *TopoFlow* model was then started as a plug-in from within *RiverTools* 3.0. It can also be started as a stand-alone application using the IDL Virtual Machine, a free tool that can be downloaded from ITT Visual Information Solutions (<http://www.ittvis.com/idl/>). Figure 5 shows the wizard panel in *TopoFlow* that is used to select which physical processes to model and which method to use

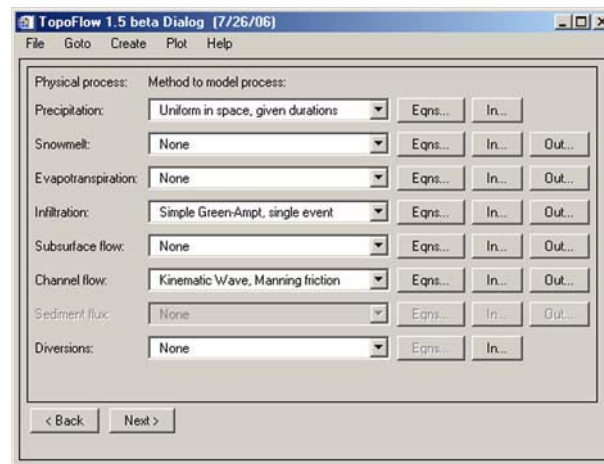


FIGURE 5 A dialog in the TopoFlow model that allows a user to select which method to use (if any) to model each hydrologic process from a droplist of choices. Once a choice has been selected, clicking on the “In...” or “Out...” buttons opens an additional dialog for entering the parameters required by that method. Clicking on the “Eqns...” button displays the set of equations that define the selected method.

for each process. Several methods are provided for modelling each hydrologic process, including both simple (e.g. degree-day, kinematic wave) and sophisticated (e.g. energy balance, dynamic wave) methods. In this example, spatially uniform rainfall with a rate of 100 [mm/hr] and a duration of 4 minutes was selected for the Precipitation process, but gridded rainfall for a fixed duration or space-time rainfall as a grid stack of rainrates and a 1D array of durations could have been used. For the channel flow process, the kinematic wave method with Manning’s formula for computing the flow velocity was selected. Clicking on the button labeled “In...” in the Channel Flow process row opened the dialog shown in Figure 6.

All of the input dialogs in TopoFlow follow this same basic template; either a scalar value can be entered in the text box or the name of a file that contains a time series, grid or grid sequence. The filenames of the previously extracted D8-based grids for flow direction and slope (from RiverTools) were entered into the top two rows of this dialog. The filenames for Manning’s n , channel bed width and channel bank angle as grids were entered in the next three rows. These were created with a preprocessing tool in TopoFlow’s Create menu that uses a contributing area grid and power-law formulas to parameterise these quantities.

If available, field measurements can be entered to automatically constrain the power-law parameters, but for this case study default settings were used. This resulted in a largest channel width of 4.1 meters, which may be too large for such a small basin (1.84 km²). The corresponding value of Manning’s n was 0.02, which may similarly be too small. A value of 0.3 was used for overland flow. For this small watershed, a uniform scalar value of 1.0 was used for the channel sinuosity. The initial flow depth was set to 0.0 for all pixels, although TopoFlow has

Variable:	Type:	Scalar or Grid Filename:	Units:
flow_codes:	Grid	North_Basin_flow.rtg	[none]
bed_slope:	Grid	North_Basin_slope.rtg	[m/m]
Manning_n:	Grid	North_Basin_chan-n.rtg	[s/m ^{1/3}]
bed_width:	Grid	North_Basin_chan-w.rtg	[meters]
bank_angle:	Grid	North_Basin_chan-a.rtg	[deg]
sinuosity:	Scalar	1.000000	[none]
init_depth:	Scalar	0.000000	[meters]

Channel process timestep: 3.000000 [seconds / timestep]

FIGURE 6 The TopoFlow dialog used to enter required input variables for the “*Kinematic Wave, Manning’s n*” method of modelling channel flow. Notice that the data type (scalar, time series, grid or grid sequence) of each variable can be selected from a droplist. If the data type is “*Grid*”, then a filename is typed into the text box. These names refer to grids that were created with preprocessing tools. Units are always shown at the right edge of the dialog.

another preprocessing tool for computing base-level channel flow depths in terms of an annual recharge rate and the other channel parameters. The channel process timestep at the bottom was set to a value of 3 seconds, as shown. This timestep was automatically estimated by TopoFlow as the largest timestep that would provide numerical stability. By clicking on the button labeled “*Out...*” in the Channel Flow process row, the dialog shown in Figure 7 was opened. This dialog allows a user to choose the type of output they want, and for which variables. TopoFlow allows user-selected output variables to be saved to files either as a time series (for one or more monitored grid cells) or as a grid stack indexed by time. The check boxes in Figure 7 indicate that a grid stack and a time series (at the basin outlet) should be created for every output variable. A sampling timestep of one minute was selected; this gives a good resolution of the output curves (e.g. *hydrograph*) but is much larger than the channel process timestep of 3 seconds that is required for numerical stability.

Once all of the input variables were set, the model was run with the infiltration process set to None. The resulting hydrograph is shown as the top curve in Figure 10. The “*Simple Green–Ampt, single event*” method was then selected from the droplist of available infiltration process methods. Clicking on the button labeled “*In...*” in the infiltration process row opened the dialog shown in Figure 8. Toward the bottom of this dialog, “*Clay loam*” was selected as the closest standard soil type and the default input variables in the dialog were updated to ones typical of this soil type. The initial value of the soil moisture, shown as θ_{i} was changed from the default of 0.1 to the value 0.35. The infiltration process timestep

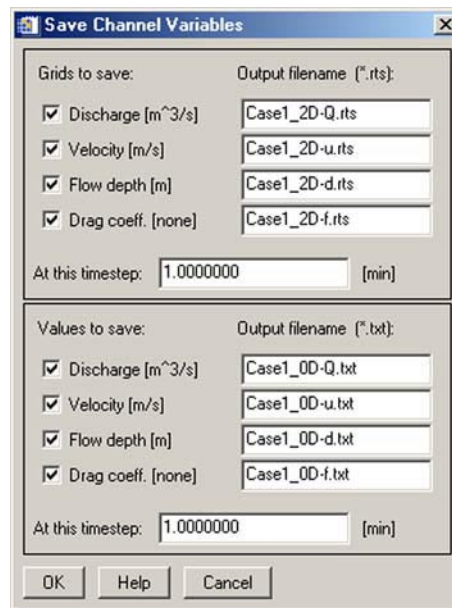


FIGURE 7 The TopoFlow dialog used to choose how model output for the channel flow process is to be saved to files. Any output variable can be saved as either a time series for all monitored grid cells (in a multi-column text file) or as a sequence of grids. The time between saved values can be specified independently of the modelling timesteps.

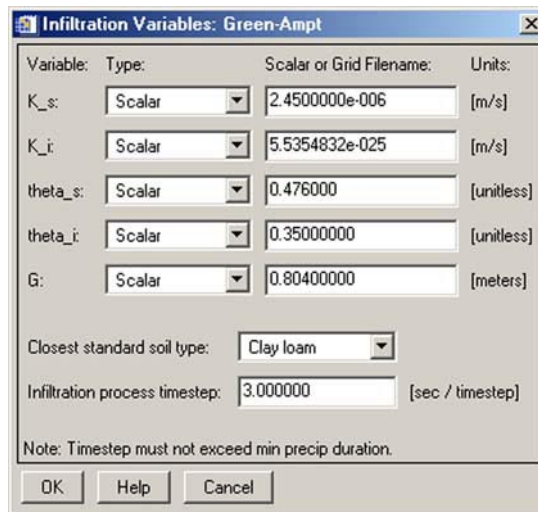


FIGURE 8 The TopoFlow dialog used to enter required input variables for the “Green–Ampt, single event” method of modelling infiltration. Here, scalars have been entered for every variable and will be used for all grid cells. Choosing an entry from the “Closest standard soil type” droplist changes the input variable defaults accordingly and can be helpful for setting parameters when other information is lacking. This is also useful for educational purposes.

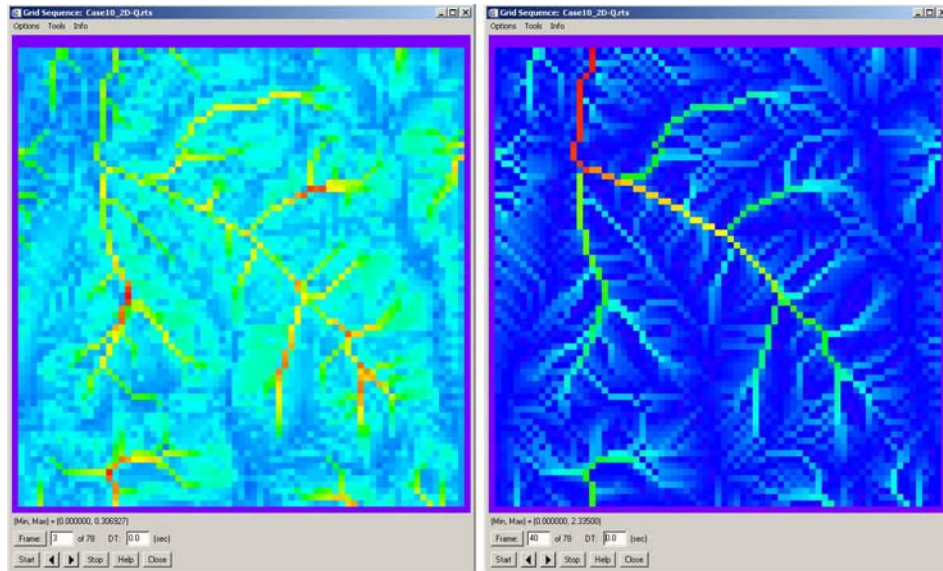


FIGURE 9 The *Display → Grid Sequence* dialog in RiverTools 3.0 can be used to view grid stacks as animations or to view/query individual frames. The frame on the left is early in a simulation, and shows flood pulses starting to converge. The frame on the right shows the spatial pattern of discharge well into the storm.

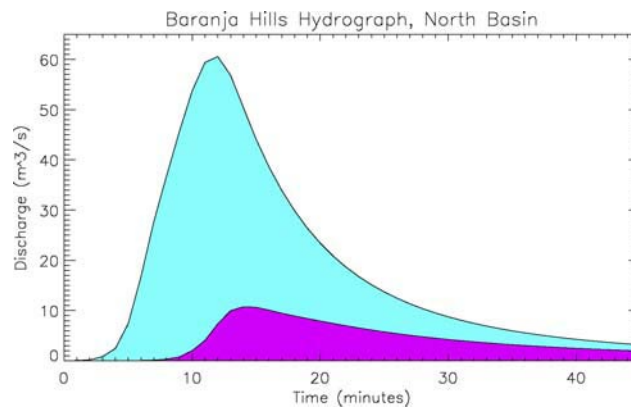


FIGURE 10 Two hydrographs, showing how the hydrologic response of the small basin differs in two simple test cases. Both cases use spatially uniform rainrate, but one also includes the effect of infiltration via the Green–Ampt method.

listed toward the bottom of the dialog was changed to 3.0 seconds per timestep, in order to match³ the time-step of the channel flow process. When the model was run again with these settings, it produced the hydrograph shown as the bottom curve in Figure 10. It can be seen that, as expected, the inclusion of infiltration resulted in a much smaller peak in the hydrograph and also caused the peak to occur somewhat later. At the end of a model run, any saved time series, such as a hydrograph, can be plotted with the *Plot* → *Function* option. Similarly, any grid stack can be visualised as a colour animation with the *Plot* → *RTS File* option. The RTS (RiverTools Sequence) file format is a simple and efficient format for storing a grid stack of data. RTS files may be used to store input data, such as space-time rainfall, or output data, such as space-time discharge or water depth. RiverTools 3.0 (see Chapter 18) has similar but more powerful visualisation and query tools, including the *Display* → *Function* tool for functions (e.g. hydrographs and profiles), and the *Display* → *Grid Sequence* tool for grid stacks (see Figure 9). The latter tool allows grid stacks to be viewed frame by frame or saved as AVI movie files. It also has several interactive tools such as (1) a Time Profile tool for instantly extracting a time series of values for any user-selected grid cell and (2) an Animated Profile tool for plotting the movement of flood waves along user-selected channels.

It is important to realise that TopoFlow can perform much more complex simulations without much additional effort at run time. It allows virtually any input variable to any process to be entered as either a scalar (constant in space and time), a time series (constant in space, variable in time), a grid (variable in space, constant in time) or a grid stack (variable in space and time). It can also handle much larger grids than the one used in this case study. Advanced programming strategies including pointers, C-like structures, dynamic data typing and efficient I/O are used throughout TopoFlow for optimal performance and the ability to handle large data sets.

6. SUMMARY POINTS

Spatially-distributed hydrologic models make direct use of many geomorphometric variables. Flow direction or aspect is used to determine connectivity, or how water moves between neighbouring grid cells, and this same flow direction is also commonly used for subsurface flow. Slope is one of the key variables needed to compute flow velocity for both overland and channelised flow. Both slope and aspect are used to compute clear-sky solar radiation, which may then be used by an energy-balance method to model rates of snowmelt and evapotranspiration. Channel lengths (between pixel centres) are used in computing flow resistance. Elevation can be used together with a lapse rate to estimate air temperature. Total contributing area can be used to determine whether overland or channelised flow is dominant in a given grid cell and can also be used together with scaling relationships to set channel geometry variables such as bed width and roughness for every grid cell.

³ It can often be set to a much larger value (minutes to hours).

One of the main advantages of spatially-distributed hydrologic models over other types of hydrological models is their ability to model the effects of human-induced change such as land use, dams, diversions, stream restoration, contaminant transport, forest fires and global warming. A truly amazing variety of problems can now be addressed with fully-spatial models that run on a standard personal computer. While much work remains in order to resolve issues such as upscaling, these models can be extremely useful if applied with an understanding of their strengths and limitations. Clearly, results do depend on grid spacing, and the greatest uncertainties occur when grid cells are larger than the hillslope scale. For small to medium-sized basins, the problem of upscaling appears to be tractable and significant progress has already been made. Note that many of the problems such as subgrid variability, modelling of momentum loss due to friction and specification of initial conditions are also encountered by fully-spatial climate and ocean models.

REMARK 5. *Spatial hydrologic models can address many types of problems that cannot be addressed with simpler models, such as those that involve the effects of human-induced changes to all or part of a watershed.*

In view of the large number of distributed models now used in hydrology and other fields, there is clearly a growing consensus that their advantages outweigh their disadvantages. A key attraction of physically-based, distributed models is that processes are modelled with parameters that have a physical meaning; note that even an effective parameter may have a well-defined physical meaning. These models also promote an integrated understanding of hydrology, rather than focusing on a particular process and neglecting others. These features combined with their visual appeal makes them very effective educational tools, especially when a variety of different methods are provided for modelling different processes, when any process can easily be turned off and when well-documented source code is made available.

IMPORTANT SOURCES

- Rivix LLC, 2004. RiverTools 3.0 User's Guide. Rivix Limited Liability Company, Broomfield, CO, 218 pp.
- Peckham, S.D., 2003. Fluvial landscape models and catchment-scale sediment transport. *Global and Planetary Change* 39 (1), 31–51.
- Blöschl, G., 2002. *Scale and Scaling in Hydrology — A Framework for Thinking and Analysis*. John Wiley, Chichester, 352 pp.
- Beven, K.J., 2000. *Rainfall-Runoff Modelling: The Primer*, 1st edition. John Wiley, New York, 360 pp.
- Beven, K.J., 1997. TOPMODEL: a critique. *Hydrological Processes* 11 (9), 1069–1086.